Discriminating dusts and dusts sources using magnetic properties and hematite:goethite ratios of surface materials and dust from North Africa, the Atlantic and Barbados.

Oldfield, F.[1], Chiverrell, R.C.[1], Lyons[2], R., Williams, E.[3], Shen, Z.[4], Bristow, C.[5], Bloemendal, J.[1,7], Torrent, J.[6], Boyle, J.F.[1]

[1] School of Environmental Sciences, University of Liverpool, Liverpool, UK.

[2] School of Geosciences, University of the Witwatersrand, Johannesburg, Private Bag 3, South Africa

[3] Department of Civil and Environmental Engineering, Massachusets Institute of Technology, Cambridge, MA 02139-4307, USA.

[4] Department of Earth & Environmental Sciences, Room 204 Blessey Hall, New Orleans, LA 70118, USA

[5] Department of Earth and Planetary Sciences, Birkbeck University of London, London WC1E 7HX

[6] Departamento de Agronomía, Universidad de Córdoba, Edificio C4, Campus de Rabanales,14071 Córdoba, Spain

[7] 2011 Cooperative Innovation Center for Arid Environment and Climate Changes, Lanzhou University, Gansu, 730000, China

Corresponding author: F. Oldfield, oldfield.f@gmail.com Tel: 44(0) 151 632 6154

Highlights

Magnetic measurements discriminate dust sources in North Africa

Bodélé Depression sediments and dusts dissimilar from measured Atlantic and Barbados dusts

Measured Atlantic and Barbados dusts from the 1970's more closely resemble those from the Sahel region.

Abstract

Magnetic measurements and Diffuse Reflectance Spectroscopy are used in an attempt to differentiate dusts and dust sources in North Africa, over the Atlantic and in Barbados. Special attention is paid to dusts and to lacustrine clay and diatomite samples from the Bodélé Depression, in view of its alleged importance in trans-Atlantic and global dust generation. The results indicate that dusts from the Bodélé depression can be distinguished from other dusts and potential sources in Niger, Chad, Burkina and Mali on the basis of their magnetic properties, notably their low magnetic concentrations, negligible frequency dependent magnetic susceptibility and distinctive IRM demagnetization characteristics. Dust from over the Atlantic and from Barbados, obtained from meshes in the 1960s and '70s have high frequency dependent susceptibility values, are quite distinctive from the Bodélé Depression samples and are more closely comparable to samples from elsewhere in the Sahara and especially the Sahel. The Diffuse Reflectance Spectroscopy data, though of limited value here, are not inconsistent with the inferences based on the magnetic measurements. Overall, the results obtained point to a wide range of sources for dusts both over North Africa itself and across the Atlantic. They do not offer support to the view that dusts from the Bodélé Depression have dominated supply across the Atlantic over the last five decades.

Key words: Magnetic measurements; Diffuse Reflectance Spectroscopy; Bodélé Depression; North Africa; Dust sources; Trans-Atlantic dust transport.

1. Introduction

Over the last decade and especially in the wake of the BodEx campaign in 2005 (BodEx, 2005), the role of the Bodélé Depression as a possible major, global dust source has received much attention. The east-west trending depression, some 500km by 150km, lies along the northern edge of the former mega-lake Chad which, at its greatest extent during the early –mid Holocene covered at least 350,000 km^2 . Within the depression, the sediments susceptible to deflation comprise mainly diatomites (Bristow et al. 2009). From a combination of modeling (Tegen et al. 2006), meteorological observations and remote sensing (Washington et al. 2003; 2005a, b), claims have been made that the Bodélé Depression may be the most important single source of dust in the atmosphere on a global scale (Washington et al. 2009). Moreover, aerosol trajectories (Ben-Ami et al. 2010) and geochemical analyses (Bristow et al. 2010) have been used to suggest that it may be a dominant source of dust and nutrients to Amazonia, mainly as a result of transport during winter months (Koren et al. 2006; Lovett, 2010). The study by Engelstaedter and Washington (2007) also reinforces the view that the Bodélé Depression is a significant hotspot for dust generation, alongside a wider range of sources in West Africa, which they claim are most active in June. Claims for the unique significance of the Bodélé Depression in dust generation have been contested recently by Crouvi et al. (2012), whose results show that dust sources in North Africa are much more widespread and diverse. They suggest that the extensive areas of mobile dunes are the dominant dust source, more important overall than the Bodélé Depression. At least one study, combining data from Meteosat-8 and surface measurements, documents a major Saharan storm drawing dust from a wide area over the Sahara and Sahel under the influence of northerly winds in March 2006 (Slingo et al. 2006). Moreover, Williams (2008) shows that satellite observations using the TOMS remote sensing instrument, data from which has been crucial in highlighting the outstanding significance of the Bodélé Depression as a dust source, are limited through blocking by upper level cirrus clouds, leading to a failure to capture the

importance of dust outbreaks from the Sahel through the action of 'haboobs', intense dust storms carried on gravity currents mainly during summer months.

Relatively little research has been focused on establishing the extent to which the characteristics of the Bodélé Depression dust sources can be used to distinguish them from other North African dust sources and from dusts collected beyond the limits of the Depression. However, Abouchami et al. (2013), using geochemical and isotopic data, show that the Belterra Clays of the Amazon basin, considered by some to be derived from eolian dusts are clearly distinguishable from material from the Bodélé Depression. Instead, they appear to have been derived from in-situ weathering. The sediments of the Bodélé Depression include extensive areas of exposed diatomites. Recognizable diatom frustules have been recovered from dusts over the Atlantic (e.g. Ehrenberg 1849; Delany et al. 1967; Romero et al. 1999). Diatomites, however, are not confined to the Bodélé Depression. Several studies (Gasse, 1987,2002; Servant and Servant, 1970) confirm how widespread and diverse are the diatom assemblages in sediments from the numerous lake basins in the Sahara-Sahel.

Previous studies confirm the value of magnetic measurements in discriminating dust sources globally (Maher, 2011), across North Africa (Lyons et al. 2010; 2012) in the North Atlantic and in Barbados (Oldfield et al. 1985). In the present paper we explore the role of magnetic measurements and Diffuse Reflectance Spectroscopy (DRS) in (i) discriminating a range of dusts and potential dust sources across the Sahara and Sahel regions, including the Bodélé Depression, (ii) allowing comparisons between the characteristics of these potential sources and those of dust samples taken from North Africa, the mid-Atlantic and Barbados and (iii) assessing the extent to which comparisons between the measured properties of the material from the Bodélé Depression and those from elsewhere are consistent with the suggestion that the Depression has been a dominant source of the dusts deposited elsewhere in N Africa, over the Atlantic and beyond.

Even where, as is often the case, it has been impossible to quantify mineral contributions from magnetic measurements, they have often proved valuable in discriminating materials on the basis of their provenance, especially where the measurements are diagnostic of distinctive environmental processes or sources (Liu et al. 2012 in press). DRS also has been used successfully for characterizing soils and sediments and linking them to environmental processes (Ji et al. 2001; Hao et al. 2009). From Liu et al. (2011), it is clear that quantitative determination of concentrations using DRS is likely to be unreliable where the forms, sources and degree of substitution and grain sizes are, as is likely to be the case here, very diverse. Use of DRS has therefore been limited to estimating the ratio between hematite and goethite in view of the likely link between the ratio and different environmental contexts and weathering regimes (Schwertman and Taylor, 1989). Goethite and hematite play an important role in controlling the colour and reflectance of potential dust sources and the dusts themselves.

2. Samples of surface materials and dusts

The total sample set upon which the present study is based comprises 245 surface materials and dusts in the following groups:

1. Surface materials collected during three field trips between 2006 and 2010. These comprise samples along transects in Mali, Niger, Burkina Faso and Chad (n = 146). Of these, 12 (Group 1a) are from the region to the east of 12^{o}E and north of 18^{o}N, from the most northerly and arid parts of Niger. These surface samples are also paired with the subset of dust samples from the same locations (Group 2a below). Samples from the field sampling in

2010 include 8 from the Bodélé Depression (Group 1b) as well as 13 samples from Chad (Group1c) that span the arid zone to the north and south of the Depression.

2. Dusts, including 34 collected along the first broadly north-south Niger transect between July and September, 2007, mainly obtained by brushing exposed, elevated surfaces on old buildings. These integrate dust fall from unknown and variable periods of time. Of these, 12 are from the most arid region of N Niger (2a). In addition, 7 samples were collected between 15.11.2007 and 14.10.2008 from Niamey, most from a previously cleaned radar dome that integrated dust fall over 3 years (2b). Dusts were also collected in 2010 from sites in Niger and Chad (2c). These comprise four that represent dust accumulation over a period of at least several months, as well as one sample (Lab. No. 88) taken during a Harmattan dust storm during the winter 2009-2010.

3. Surface materials and dusts from the Bodélé Depression collected during the BodEx campaign in 2005 (n = 18). The mass of many of these samples is <0.5g.

4. Dust samples from Barbados and mid-Atlantic (n = 33). 15 of the samples from Barbados were taken between October 1966 and July 1969 by means of nylon mesh panels and are among those included in Oldfield et al. (1985) and referred to below as group 4a. They include both red 'summer' dusts and grey 'winter' dusts. An additional mesh sample was taken in July 1970 and this was the only sample from Barbados available for inclusion in the suite of measurements upon which Figure 9 is based. All but one of the remainder come from two sets of dusts obtained from mesh samplers on board ship. One set is referred to in Oldfield et al. (1985) and the other was provided by R. Chester for which precise location other than 'mid-Atlantic' can no longer be established. Both were obtained during the 1970s and, along with an additional mesh sample taken on the Glomar Challenger in March 1975, constitute group 4b.

The samples from North Africa (Groups 1-3) are associated with a marked range of climatic settings with a gradation of weathering regimes. This mainly relates to the strong, broadly north-to-south rainfall gradient across North Africa. Rainfall ranges from <30 mm/yr in the hyper-arid north of Niger and Chad to around 1000 mm/yr in southern Niger and Mali. In general, rainfall increases sharply south of ~15°N where the climate is influenced by the West African monsoonal rains, which are driven by the annual migration of the Intertropical Convergence Zone (ITCZ) (Hastenrath, 1991). Surface samples are mostly associated with Quaternary playa deposits, dunes and laterites (Schlüter, 2006).
Surface deflation and dust production are driven by two dominant wind systems–the north easterly winter Harmattan winds and the south westerly summer monsoon winds (Hastenrath, 1988). The Harmattan winds typically occur from October to April and transport vast quantities of mineral dust southwest from the Sahara towards the Gulf of Guinea and across the Atlantic (McTainsh and Walker, 1982). Summer winds, which also have the potential to transport vast quantities of material, commonly precede the onset of westward moving storms (Drees et al., 1993).

Figure 1 shows the location of the sampling sites in N Africa.

Samples in groups 1 and 2 include some that form part of the data upon which previous publications by Lyons et al. (2010; 2012) are based. Those from Chad, including the Bodélé Depression itself, and from Burkina Faso, as well as the dusts in Group 2b and 2c are considered here for the first time. With only two exceptions, (both supplied by J M Prospero, one from Barbados and one from the mid-Atlantic) samples in Group 4 have not been

available for analysis beyond routine magnetic measurements completed several years before the present study began.

Figure and Table captions and labels link the data plotted to the above 4 groups.

3. Methods

3.1 Magnetic measurements

All samples in Groups 1 to 3 and 4b were subject to a standard range of magnetic measurements comprising low field susceptibility at both low (0.47 kHz; χ_{LF}) and high (4.7 kHz; χ_{HF}) frequencies, leading to the calculation of the frequency dependent susceptibility as the difference between the two, expressed here as a mass specific value (χ_{FD}). Anhysteretic Remanent Magnetisation (ARM), expressed as susceptibility of ARM (χ_{ARM}); 'Saturation' (1T) Isothermal Remanent Magnetisation (SIRM) followed by DC reverse field demagnetisation in fields of -20mT, -40mT, -100mT and -300mT. This sequence of measurements has generally provided a good basis for the initial magnetic characterization and discrimination of sample sets, whether of sediments (Oldfield, 2012), soils (Hao et al. 2008) or dusts (Lyons et al. 2012). Details of instrumentation, methods and measurements are given in Lyons et al. (2010) and their interpretation is considered in more detail in Walden et al. (1999) and Maher (2011). The samples in group 4a were measured before equipment able to deliver a DC field up to 1T was available. For these samples, the peak DC field was 830mT and the highest reverse field used was -200mT.

Subsets of samples from groups 1-3 above were used for additional measurements. Stepwise IRM acquisition using 31 fields between 15mT and 1T and subsequent model-based deconvolution (Heslop et al. 2002) were used to provide more detailed information on the remanence carriers present. An attempt was made to quantify growth of high field IRM's up to 7T with a view to discriminating between contributions from hematite and goethite (Hao et al. 2009). The high field (0.8T) magnetization behavior of samples over the temperature range 40–700°C, at a heating rate of 30°C min^{-1} in air, was measured using a Curie Balance and a Magnetic Measurements Variable Field Translation Balance (VFTB) with a view to establishing the main magnetic minerals present in each sample. Magnetic hysteresis measurements were also performed using a VFTB. Samples were magnetized in fields ranging from 1 T to -1 T. The hysteresis loops were slope corrected for diamagnetic and paramagnetic contributions using the RockMag Analyzer 1.0 software (Leonhardt, 2006), which assumes that all remanence carriers are saturated in a field of 0.8 T.

Susceptibility measurements for many samples, including those with low mass from the Bodélé Depression, had values within the range significantly affected by the diamagnetic effect of packing material (plastic 'cling' film) and sample holder. Repeat measurements and adjustment for diamagnetic effects allowed estimates of susceptibility values, but the remaining uncertainty was too great to permit their use in quotient calculations using χ_{LF} as the denominator.

3.2 Diffuse Reflectance Spectroscopy

To establish the ratio between hematite and goethite concentrations in the samples we used diffuse reflectance UV-VIS spectroscopy (DRS) (Torrent and Barron, 2002; Torrent et al., 2007). A representative selection of samples from groups 1-3 were dried, powdered (<10

μm), dried and pressed to pellets using a 15 ton hydraulic press, before collection of the DRSpectra. The DRSpectra were recorded from 190 to 1100 nm at 0.5-nm steps at a scan rate of 30 nm min^{-1}, using a Thermo Evolution 300 UV-Vis Spectrophotometer equipped with a Praying Mantis Diffuse Reflectance Accessory (Thermo Scientific) that uses all-aluminium coated optics rather than traditional integrating spheres allowing an extended optical range. The Praying Mantis allows a diffuse reflectance measurement on samples as small as 3 mm in diameter and 1 mm thickness. For each sample the spectrum of reflectance (R) was transformed using Kubelka-Munk (K-M) remission function [$F(R) = (1-R)^2/2R$)]. Researchers have varyingly then either used the 1st (Deaton & Balsam, 1991) or 2nd (Scheinost et al. 1998; Torrent et al. 2007) derivatives of F(R) to characterise the iron oxides present. We have used both methods and only where both confirm the presence of pronounced peaks for hematite (1st derivative ~560nm) and/or goethite (1st derivative ~435nm) have we then calculated ratios. Our analyses are comparable with previous work on hematite and goethite concentrations in sediments; this we assessed by analysing a training set of 25 soils ($r^2 = 0.88$) from the Mediterranean region with hematite and goethite concentrations determined by x-ray diffraction (Torrent and Barron, 2002).

3.3 Particle size separation

A small subset of representative samples from groups 1-3 above was separated into particle size fractions using a combination of disaggregation, sieving and pipetting as described in Lyons et al. (2010; 2012). Once obtained, fractions were freeze dried. Wherever subsequent sample sizes permitted, these were subject to the range of standard magnetic measurements noted above. Maher et al. (2010) follow Pye (1989) in suggesting that dust transport involving long-term suspension is generally limited to particles <20μm. They also note that particles crossing the Atlantic have a mass median diameter between 1.5 μm and 3 μm. In light of these observations, the data presented here are limited to particles <16 μm, with special focus on those <4 μm.

4. Results

Figure 2 shows examples of hysteresis loops and thermomagnetic experiments representative of samples from the most arid part of the transect of samples from N Niger and Chad, the Bodélé Depression and the dust samples collected from Niger and Chad in 2010. The main hysteresis loops are corrected for paramagnetism; the uncorrected loops are shown as insets.

The low mass (<0.3g) and minimal concentrations of ferrimagnetic minerals in some of the critical samples, for example the dusts from the Bodélé Depression, have seriously limited the range of routine magnetic properties that can be reliably used as a basis for comparing the samples from the Bodélé Depression with those from other parts of the Sahara and Sahel, and with the dusts from the Atlantic and Barbados. For the weakest and smallest samples, ARM values lie within the noise range of the Molspin Magnetometer. χ_{ARM} values and quotients based on them have therefore not been used in the present analysis of the results.

Although the minimal susceptibility readings have posed problems for calculating χ_{LF} and χ_{HF} and precluded use of quotients involving χ_{LF} measurements, especially where these latter lie in the same range as the corrections for diamagnetism, repeat measurements, up to 10 at each frequency, have made it possible to calculate χ_{FD} values with acceptable accuracy and precision, since the values at each frequency are equally affected by diamagnetic and paramagnetic effects.

In light of the above constraints, the range of routine measurements used in the present analysis is limited to the results obtained from χ_{FD} and IRM measurements. Changes in instrumentation, peak DC field and chosen reverse fields since 1985 also mean that of these measurements, only χ_{FD} values are common to the whole sample set. Figures 3a and 3b plot, as box-whisker graphs, the χ_{FD} values for all the bulk surface and dust samples used in the present study. In the case of the values for bulk samples of potential surface sources (Figure 3a), the narrow range for the Bodélé samples lies at the low extreme of the total set, overlapping with only a small minority of the other sample sets. The aggregate value for the Bodélé dusts (Figure 3b) after 10 measurements of all 8 samples at each frequency is zero, distinguishing them from all the other dust sample sets.

Figure 4 records the χ_{FD} values for all the particle size fractions measured. In it, histograms A and C plot data from surface materials, B and F, data from dusts, taken on the first two transects (Lyons et al. 2010; 2012). Plots D and E (Samples A and B) relate to surface samples from northern Niger taken on the third transect; for each sample, material from 4 samples was aggregated before disaggregation. No measurable material between 4 μm and 16 μm was present in either case. Plot G represents aggregate data from Bodélé Depression surface materials (see figure caption). These results show that for all particle sizes up to 16μm, the χ_{FD} values for the Bodélé samples lie below those for all the other sample sets in every case where measurements could be made.

Table 1 shows the SIRM and DC demagnetization values (reverse field) results (listed as 'S' percentage values for each reverse field) for all the samples from the Bodélé Depression. Of the surface samples listed, three (CH39: Angamma Delta and Bulk samples Lab. Nos. 83 (44D) and 86 (54B)) are atypical. CH39 lies outside the range of any other sample considered here in terms of the properties used in Figures 8 and 9; 44D and 54B are dominated by hard remanence minerals which give rise to 'S' values that are also well outside the range of any other samples in the whole set. For these reasons and because they represent surfaces less amenable to deflation, they have been excluded from all subsequent Figures and Tables. Within these, the Bodélé Depression samples used include the clayey lacustrine sediments, diatomites and dune material.

Table 2 gives the range of SIRM values for all the sample groups. The range of values for the Bodélé surface samples is below the range for all the dusts and all the surfaces except for those from Niger and Chad. Values for the Bodélé Depression dusts overlap the range of values for all the dust sample sets except for those from the 1985 mid-Atlantic set.

In the case of several of the samples from the Sahel region of Mali, it was possible to characterise stepwise acquisition of IRM between 1T and 7T (Lyons et al. 2010) and, thereby infer dominance of the highfield remanence by hematite. By contrast, in most of the samples from the Sahara region, including all those from the Bodélé Depression, remanence acquired above 1T was within the noise range of the equipment. Consequently, no inferences regarding the relative contributions of hematite and goethite to high field remanence were obtainable from the magnetic measurements.

Figures 5-7 present the results of stepwise IRM acquisition up to 1T and subsequent model based deconvolution (Heslop et al. 2002) for selected representative samples. In the absence of reliable quotient values based on χ_{ARM} and χ_{LF} measurements for many of the critical samples, this technique, by characterizing the coercivity spectra of the remanence carriers in each sample, provides one of the best ways of identifying parameters likely to discriminate between sample sets. Figure 5 shows results for representative samples from the Sahara region of Niger and Chad outside the Bodélé Depression, Figure 6 for sample 80 from the

Bodélé Depression itself and Figure 7 for a series of dust samples from Niger and Chad (Group 2 above). Table 3 presents the deconvolution results for the samples from all three Figures. For the Bodélé Depression samples, the $B_{1/2}$ values for the lowest coercivity component lie between 45mT and 63mT; for all the other samples, whether surface materials or dusts, the $B_{1/2}$ values for the lowest coercivity component range from 14mT to 47mT .Figures 5-7 and their summary analysis in Table 3 suggest that the reverse field results derived from the DC demagnetization of the SIRM may provide a useful basis for discriminating between sample sets, especially where, as in the case of the individual Bodélé Depression dust samples, weak signals have made the differences in IRM over the close field intervals between successive acquisition measurement unreliable for deriving coherent acquisition plots. These results therefore establish the rationale for the subsequent figures based on parameters derived from reverse field IRM measurements.

Figures 8 and 9 show the cross-plots of two parameters derived from the reverse field measurements. The 'L' parameter is obtained by dividing the un-reversed IRM at -300mT by that un-reversed at -100mT. As used here (Hao et al. 2008) it is a modification of that proposed by Liu et al. (2007) and is designed to demonstrate differences in the characteristics of the hard remanence (mainly imperfect antiferromagnetic minerals and predominantly hematite) portion of the total assemblage of magnetic minerals contribution to the SIRM. The F parameter, defined and used here for the first time, is the difference between IRM_{-20mT} and IRM_{-40mT}, divided by the difference between SIRM and $IRM_{-40mT.}$ It is designed to reveal differences in the 'soft' remanence ferrimagnetic minerals (magnetite and maghemite) contributing to the SIRM. Figure 8 shows the cross plot from the Bodélé Depression samples. The oval loop encloses the dusts and bulk sediment samples, the rectangle encloses, in addition, the surface lake sediment samples from the BodEx set as well as the particle size samples from 0 – 2 μm. Only the dune samples and coarser size fractions lie outside these envelopes. Figure 9 uses the same cross-plot to compare the values for the Bodélé Depression samples within the oval loop and the rectangle with those for other sample sets from N Africa, the mid-Atlantic and Barbados.

DRS spectra were obtained for 34 surface samples from the Bodélé Depression. These included all the bulk samples from Groups 1b and 3 as well as a series of particle sized subsamples. Only three samples, two identified previously as atypically red in colour and excluded from the sets of magnetic measurements in the preceding figures and tables, produced discernible DRS peaks reflective of hematite and/or goethite. The remaining 31 samples of dune material, lacustrine clays and diatomites, all shown by the measurements summarised above to be extremely poor in magnetic minerals, fell below the detection limits for both minerals. By contrast, the 5 tiny dust samples obtained during the BodEx campaign all recorded measurable quantities of hematite using both approaches to calculation. The lack of a first derivative peak in the DRSpectra at ~430nm suggests that Goethite is not detectable in these samples. 51 additional surface samples and dusts taken from outside the Bodélé Depression were also analysed. These spanned the full range of material obtained from the Sahel and Sahara (Lyons et al. 2010; 2012). Of these, 41 provided measurable values using both methods. All had measurable hematite peaks, but only 16 recorded goethite.

5. Discussion

5.1 Hysteresis and thermomagnetic properties

The previous studies spanned a wide range of environments across the Sahel and Sahara (Lyons et al. 2010; 2012), but lacked plots derived from magnetic hysteresis and thermomagnetic experiments for samples from the arid portions of Chad and Niger. These are the areas where the climatic regime is most similar to that prevailing over the Bodélé Depression. Consideration of representative samples from this region is therefore included in this part of the discussion.

Figures 2a and 2b illustrate the range of plots from the most arid regions sampled. In the case of sample 47 with the highest value for χ_{LF} from that part of the data set, there is a definable, narrow hysteresis loop closing below 300mT with very little increase in slope-corrected M above this, confirming that ferrimagnetic minerals dominate the magnetic signature. The thermomagnetic plot shows a Curie temperature close to that of magnetite at 580^{o}C. By contrast sample 45, one of the weakest in the set, has an uncorrected hysteresis plot with no clear loop within a trend of increasing magnetization with increasing field, confirming dominance by paramagnetic minerals. The corrected loop is slightly wasp-waisted; this and the continued positive slope are both indications of hematite and/or goethite. The thermomagnetic plot, typical of paramagnetic material, shows a smooth decline in magnetization with temperature and no detectable inflexion from room temperature to 700^{o}C. Figure 2c represents a typical sample from the potentially deflatable part of the Bodélé Depression. The uncorrected loop points to dominance by paramagnetic minerals. The thermomagnetic curve is largely dominated by paramagnetic minerals, except in so far as there is a slight suggestion of a magnetite-type Curie temperature around 580^{o}C and of some conversion to a weaker magnetic phase above this, given the reduced values in the cooling curve. Figure 2d is one of 5 plots for dust samples collected from Niger and Chad. It shows clearly the growth of a new magnetic phase above 400^{o}C probably as a result of the combustion of organic matter within the sample. As a consequence, the cooling curve rises well above the heating curve, a feature common to all the dusts measured. This means that the Curie temperature represents a newly formed ferrimagnetic phase during heating, rather than the original mineral content.

The results as a whole point to the importance of paramagnetic contributions to the magnetic properties of the samples from the most arid parts of the Sahara. Hysteresis and thermomagnetic measurements (see also Lyons et al. 2010) fail to provide a basis for discrimination between the Bodélé Depression materials and those from elsewhere in the arid Sahara.

5.2 The Bodélé Depression samples

From the results summarised in Table 1, it is possible to assess the range of variation in the magnetic properties of surface materials within the Depression and to compare these with the 5 dust samples that show remarkable uniformity in reverse field ratios despite an almost twofold variation in SIRM. The dusts therefore appear to vary only in terms of magnetic concentrations, not in terms of the magnetic mineral assemblages present. Of the surface samples obtained during the BodEx experiment, as noted above, the only sample falling well outside the dust envelope of values is CH39 from the Angamma Delta (Sample CH39, Table 1). The SIRM is over 20 times higher than the most magnetic of the dusts and the reverse field values show a stronger degree of reversal at each step. All the other samples show broadly similar reverse field values close to the range for the dusts, despite the SIRM values being, on average, only about a third of those of the dusts.

Of the 8 samples from the Depression taken in 2010 (Table 1), two (Lab. Nos. 83(Field sample No.44D) and 86 (54B)) have higher SIRMs and the reverse field values are indicative of a much higher percentage of imperfect antiferromagnetic minerals (hematite and possibly goethite) These samples, along with that from the Angamma Delta noted above, are red in colour and are not thought to contribute significantly to dusts from the Depression (Bristow et al. 2009). Sample 84 (51), with higher SIRM and higher reverse field percentages at each step, also falls somewhat outside the range of the others. These samples have been excluded from Figures 8 and 9. The remaining 5 bulk samples (79, 80, 81, 82 and 85) form a coherent group, but differ from the BodEx surface materials by having even lower SIRM values (<23 as against values of 49.9.- 117.2 x $10^{-5}Am^2kg^{-1}$) .

Of the various samples obtained from the Depression, only those obtained in 2010 included enough material for particle size separation. The results for the four samples used show rather uniform reverse field values for the <2μm fraction which forms the bulk of each sample. Despite very low SIRM values, the reverse field percentages, especially for samples 80 (44), 81 (44B) and 82 (44C), are quite similar to those for the dusts. The magnetic properties of the coarser fractions are more varied between samples, and especially above 4μm, their high (-100mT and -300mT) reverse field percentage values diverge more strongly from those of the dusts. In no sample was sufficient material >16μm obtained for individual measurement.

From the tabulated results and the cross-plot shown in Figure 8, it appears that once a small number of atypical, mostly red coloured samples from deltaic or other localised environments are excluded because of their extreme magnetic properties and the unlikelihood that they would have yielded significant amounts of deflatable material, similar magnetic mineral assemblages can be recognised in 85% of the dusts and grey-white surface materials despite major differences in their magnetic mineral concentrations. Although there may be some contribution to the dusts from sources represented by the outlier samples excluded from the Figures and Tables, as well as from areas outside the Depression, these differences in concentration can be mainly explained by the processes of winnowing, selective re-suspension and sorting taking place in the highly dynamic surface environment of the Depression. Together, these processes could readily lead to enrichment or dilution of a rather uniform assemblage of magnetic minerals depending on the ratio between them and the diatom frustules which form the main matrix within much of the dried up lake sediments. A similar magnetic enrichment of the dusts relative to nearby sources is also apparent in the samples from Niger reported in Lyons et al. (2012) as well as in the comparisons between surface and dust values of χ_{FD} given in Figure 3.

5.3 Discriminating magnetic properties

The data shown in Figures 3a and 3b and Tables 1 and 2 confirm that in terms of magnetic concentrations, the low values for the samples from the Bodélé Depression generally place them either outside the range of all the other samples measured or at the low extreme. Previous results from N Africa (Lyons et al. 2010; 2012) have shown that variations in both χ_{LF} and χ_{FD} values are linked to north-south climatic gradients. To the south, pedogenesis has led to higher concentrations of fine-grained, secondary ferrimagnetic minerals as a result of the higher rainfall and consequent higher levels of chemical weathering (cf Maher and Thompson 1995; Balsam et al. 2011). The gradient in secondary magnetic mineral concentrations was relatively consistent in both the surface materials and in sampled dusts, despite the complications arising from diverse substrates and the possible legacy from previous weathering regimes, especially during the early-mid Holocene (Hoelzmann et al. 2004). Thus the area of the Sahel, with rainfall over 200mm p.a. tends to have soils with

higher χ_{LF} and χ_{FD} values than those prevailing in the more arid Saharan regions to the north. This gradient appeared clearly in the southwest to northeast transects of both the surface and dust samples upon which the previously published papers by Lyons et al. (2010 and 2012) were based. Additional samples from the transects in 2010 are more difficult to fit into this scheme as both the surface materials (Fig. 3a) and dusts (Fig. 3b) show strong overlap between the Sahel and Sahara sample sets. One possible complicating factor, especially for samples taken along the transect to the west of Niamey and into Burkina Faso, is the prevalence of eroding laterite close to many of the sample sites. It is therefore possible that some surface materials include contributions from material unrelated to contemporary or recent weathering regimes.

The range of values for the dusts is, in every case where direct comparisons can be made, significantly higher than for the surface materials. This is especially the case for the sample sets from sites within the zone of transition between Sahel and Sahara and those from west of 12°E despite the fact that both sets lie within the zone of dominant dust transport from the Sahara to the south and west (Washington et al. 2003; 2005a and b). From these comparisons, we infer that the surface samples are depleted, not only in finer particle sizes, but more specifically in those containing magnetically fine grained ferrimagnets carrying the χ_{FD} signature. Despite any possible depletion in the fine, χ_{FD} carrying particles, the χ_{FD} values in the surface sands outside the Bodélé Depression are consistently higher than in typical samples from the Depression itself (Fig. 3a), thus increasing the significance of the contrast between the two types of source.

Many repeat measurements of χ_{LF} and χ_{FD} for both the dust and surface samples from the Bodélé Depression confirm that the magnetic properties of the bulk samples lack any measurable χ_{FD} component despite their dominance by clay and fine silt size particles. The lowest χ_{FD} values for some of the bulk surface samples from the Sahara and Sahel (Fig. 3a) come close to those from the Bodélé Depression samples and so do not alone allow a distinction between these extreme samples and those from the Bodélé Depression, though the particle size based measurements (Fig. 4) show that for any given grade, the Bodélé Depression samples have the lowest values. The Bodélé Depression dusts also differ significantly in most respects from all the other dusts included in the present data set, whether from N Africa, Barbados or the Atlantic (Fig. 3b), although it should be noted that all the samples from beyond N Africa date from the mid to late 1960s and 1970s. The possibility that changes in wind strength and direction since that time may be responsible for the differences between these dusts and Bodélé Depression dusts seems unlikely in light of the results of Vermeesch et al. (2012). Based on measurements of dune mobility they conclude that there has been little change in dominant wind strength or direction in the area around the Bodélé Depression over the last 45 years. The differences in magnetic properties may however reflect a well-documented period of more severe Sahel drought and deflation during the late 1960s and 1970s than has prevailed over recent years (NCEP, 1994; Prospero and Nees, 1977). It is also important to note that Barbados lies to the north of Amazonia and of the equatorial path across the Atlantic inferred for the dominantly winter dusts from the Bodélé Depression.

Unlike the χ_{FD} values, the SIRM values for the Bodélé Depression dusts (Table 2) overlap those for most of the other data sets, prompting a need to consider in more detail the comparison between the dusts and surface materials from the Depression itself, as well as between the Bodélé Depression samples and those from the remainder of the Sahara/Sahel.

Despite the range of 'L' values for the diatomites, clay size sediments and dune material from Bodélé Depression samples, Figure 9 shows, largely on the basis of the 'F' values, little overlap

between those and all the other samples. No samples from outside the Depression fall within the oval loop that encloses the dusts and bulk sediment samples from the Depression. The rectangle overlaps with only 12% of the non-Bodélé samples. These indications are consistent with the distinction between the Bodélé Depression samples and the rest made in the IRM acquisition plots. They confirm the value of the F parameter in discriminating between the Bodélé Depression samples and all others measured. Along with the IRM acquisition plots, they suggest that there is a distinction between the Bodélé Depression samples and the rest in the softest IRM phase. The very low magnetic concentrations make it impossible from the present measurements to determine whether the magnetically softest component in the non-Depression samples denotes multidomain or fine viscous minerals. The range of $B_{1/2}$ values for the dominant, low coercivity, component of the Bodélé Depression samples (Fig. 6 and Table 3) points to a distinctively different magnetic grain size for the ferrimagnetic (magnetite + maghemite) minerals present, with the samples from the Depression probably including a higher proportion of stable single domain grains. This is compatible with, but does not prove the survival of low concentrations of magnetite formed within the cells of magnetotactic bacteria in the sediments (Oldfield, 2012). The values fall within the range ascribed to bacterial magnetite by Heslop et al. (2002) though the low concentrations may reflect some diagenetic loss (Shi et al. 2011).

The only sample set that overlaps significantly with the values for Bodélé Depression samples in Figure 9 is the group of Atlantic dusts provided by R. Chester, 50% of which lie within the Bodélé rectangle. They can, however be clearly distinguished from the Bodélé material on the basis of the χ_{FD} measurements which, for the dusts in question, are between 3 and 200 times higher than the highest measurement from the Depression. These higher values link all the measured dusts from beyond North Africa mainly to those from outside the Bodélé Depression. This conclusion accords well with the results of Crouvi et al. (2012) based on observations over the period 2006 to 2008. Using data on the number of days with dust storms, and high-speed wind events, along with detailed mapping of soil types and geomorphic units they conclude that mobile dunes are the major source of dusts in the region between 20'W–45"E and 5'N–40"N.

5.4 Diffuse Reflectance Spectroscopy

Given the very few reliable data from the Bodélé Depression samples, the results from the DRS measurements are of only limited value. The presence of detectable hematite in the dust samples is compatible with the presence of higher magnetic concentrations in these samples than in the typical surface materials.

6. Conclusions

1. Variations in the magnetic properties of the samples of clay size sediments, diatomites, dune material and dusts from the Bodélé Depression reflect variations in particle size assemblages and, above all, different degrees of dilution by non-magnetic matrix (e.g. diatoms). These differences have probably resulted from processes such as selective suspension and winnowing.
2. Despite these differences, the magnetic properties of the sediments and dusts from the Depression are sufficiently distinctive to allow their discrimination from virtually all the dust samples measured, as well as all the potential surface sources. The key properties for discrimination are χ_{FD} and the newly defined 'F' parameter. The only possible exceptions are the 1970's dusts from over the Atlantic provided by R. Chester which include several that resemble material from the Depression in terms of 'F' and 'L' ratios, but differ from them by having much higher χ_{FD} values.

3. Surface samples from much of the Sahara and Sahel outside the Bodélé Depression are strongly depleted in fines except for small fractional volumes of clay size particles. They therefore have much lower χ_{FD} values than do dust samples from nearby sites. Despite their depleted nature, these surface samples from outside the Bodélé Depression still have χ_{FD} values higher than those for typical samples from the Depression itself.
4. The dust samples obtained during the 1960s and 1970s from the Atlantic and Barbados have consistently higher χ_{FD} values than those from the surfaces and dusts of the Depression and are more akin to dust samples from outside the Depression, both from the Sahel and parts of the Sahara. These results do not preclude contributions from the Depression to any of the dusts measured, especially in the case of those from over the Atlantic. Nor do they rule out the possibility that the Bodélé Depression has been the largest single source of trans-Atlantic dust to Amazonia in the last decades. Nevertheless, they fail to provide support for the view that the Depression has dominated dust supply over and beyond the equatorial Atlantic. They are much more consistent with the results of Crouvi et al. (2012) who show that the main dust sources are more extensive and diverse.
5. The present approach holds out the promise of establishing the likely present day role of dusts from the Bodélé Depression relative to those from elsewhere in N Africa, provided sufficiently large dust samples can be obtained from over the mid-Atlantic and from South/Central America.

6. Acknowledgements

We are especially grateful to Bob Jude, Mike O'Connor and Danielle Alderson who completed many of the magnetic measurements reported here and to Alan Henderson for particle size separation. We are also grateful to Dr. J.M. Prospero for his interest and advice, as well as for providing 2 mesh samples, one from Barbados, one from the Atlantic and to N. Basavaiah for the measurements on the Atlantic dust samples provided by R. Chester. Dr. W.L. Balsam's comments on an earlier draft are also much appreciated.

7. References

Abouchami, W., Näthe K., Kumar A., Galer S., Jochum K.P., Williams E., Horbe A., Rosa J., Balsam W., Adams D., Mezger K., Andreae M.O., 2013 (in press). Geochemical and isotopic characterization of the Bodélé Depression dust source and implications for transatlantic dust transport to the Amazon Basin. Earth and Planetary Science Letters.

Balsam W.L., Ellwood B.B., Ji J. Williams E.R., Long X., El Hassani A., 2011. Magnetic susceptibility as a proxy for rainfall: Worldwide data from tropical and temperate climates. Quaternary Science Reviews 30, 2732-2744.

Ben-Ami Y., Koren I., Rudich Y., Artaxo P., Martin S.T., Andreae, 2010.Transport of Saharan dust from the Bodélé Depression to the Amazon Basin: a case study. Atmospheric. Chemistry and Physics Discussion 10, 4345–4370.

BodEx, 2005. A multidisciplinary study of the 'dustiest place on earth' http://www.geog.ox.ac.uk/research/climate/projects/bodex/index.html

Boyle J.F., 2000. Rapid element analysis of sediment samples by isotope source XRF. Journal of Paleolimnology 23, 213-221.

Bristow C. S., Drake N., Armitage S., 2009. Deflation in the dustiest place on Earth: The Bodélé Depression, Chad. Geomorphology 105**,** 50-58.

Bristow C. S., Hudson-Edwards K. A., Chappell A., 2010. Fertilizing the Amazon and equatorial Atlantic with West African dust. Geophysical Research Letters 37, L14807 doi:10.1029/2010GL043486.

Crouvi O., Schepanski K., Amit R., Gillespie A.R., Enzel Y., 2012. Multiple dust sources in the Sahara Desert: The importance of sand dunes. Geophysical Research Letters 39, L13401, doi:10.1029/2012GL052145, 2012

Deaton B.C., Balsam W.L., 1991. Visible spectroscopy - a rapid method for determining hematite and goethite concentration in geological materials. Journal of Sedimentary Petrolology 61, 628 – 632.

Delaney A.C., Delany A.C., Parkin D.W., Griffin J.J., Godlberg E.D., Reiman, B.E.F., 1967. Airborne dust collected at Barbados. Geochimica and Cosmochimica Acta 31, 885-909.

Drees L.R., Manu A., WildingL.P., 1993. Characteristics of aeolian dusts in Niger, West Africa. Geoderma 59, 213-233.

Engelstaedter, S. , Washington, R., 2007. Atmospheric controls on the annual cycle of North African dust. Journal of Geophysical Research 112, D03103, doi: 10.1029/2006JD00719.

Ehrenberg, C.G., 1849. Passat-Staub und Blut-Regen. Academie der Wissenschaften, Berlin , 229pp.

Gasse F., 1987. Diatoms for reconstructing palaeoenvironments and paleohydrology in tropical semi-arid zones. Hydrobiologia 154, 127-163.

Gasse F., 2002. Diatom-inferred salinity and carbonate oxygen isotopes in Holocene waterbodies of the western Sahara and Sahel (Africa). Quaternary Science Reviews 21, 737-767.

Hao Q., Oldfield F., Bloemendal J., Guo, Z., 2008. The magnetic properties of loess and palaeosol samples from the Chinese Loess Plateau spanning the last 22 million years Palaeogeography, Palaeoclimatology, Palaeoecology 260, 389-404.

Hao Q.,Oldfield F., Bloemendal J., Torrent J.. Guo Z. 2009. The record of changing hematite and goethite accumulation over the last 22 Ma on the Chinese Loess Plateau, from magnetic measurements and Diffuse Reflectance Spectroscopy. Journal of Geophysical Research 114,B12101, doi:10.1029/2009JB006604.

Hastenrath S., 1991. Climate Dynamics of the Tropics, Kluwer Academic Publications, Dordrecht, Netherlands, pp 488.

Ji J.F., Balsam W., Chen J., 2001. Mineralogic and climatic interpretations of the Luochuan Loess Section (China) based on diffuse reflectance spectrophotometry.
Quaternary Research 56, 23-30.

Heslop D., Dekkers M.J., Kruiver P.P., van Oorschot H.M., 2002. Analysis of isothermal remanent magnetization acquisition curves using the expectation-maximization algorithm. Geophysical Journal International 148, 58-64.

Koren I., Kaufman Y.J., Washington R., Todd M.C., Rudich Y., Martins J.V., Rosenfeld, D., 2006. The Bodélé depression: a single spot in the Sahara that provides most of the mineral dust to the Amazon forest. Environmental Research Letters 1 doi:10.1088/1748-9326/1/1/014005

Leonhardt R., 2006. Analyzing rock magnetic measurements: The RockMag analyzer software 1.0, Computers and Geosciences 32, 1420–1431, doi:10.1016/j.cageo. 2006.01.006.

Liu Q.S., Robert A.P., Torrent J., Horng C., Larrasoana J.C., 2007a. What do the HIRM and S-ratio parameters really measure in environmental magnetism? Geochemistry Geophysics Geosystems 8, Q09011. doi:10.1029/2007GC001717.

Liu, Q.S., Torrent, J., Barrón, V., Duan, Z.Q., Bloemendal, J., 2011. Quantification of hematite from the visible diffuse reflectance spectrum: effects of aluminium substitution and grain morphology. Clay Minerals 46, 137-147.

Liu Q., Roberts A.P., Larrasoana J.C., Banerjee S.K., Guyodo Y., Tauxe L. , Oldfield, F., 2012. Environmental Magnetism: Principles and Applications. Reviews of Geophysics 50,doi:10.1029/2012RG000393

Lovett R., 2010. African dust keeps Amazon blooming. Nature doi:10.1038/news.2010.396

Lyons R., Oldfield F., Williams E., 2010. Mineral magnetic properties of surface soils and sands across four North African transects and links to climatic gradients. Geochemistry, Geophysics, Geosystems 11,doi:10.1029/2010 GC003183

Lyons R., Oldfield F. Williams E., 2012. The possible role of magnetic measurements in the discrimination of Sahara/Sahel dust sources. Earth Surface Processes and Landforms. DOI: 10.1002/esp.2268,xv

Maher, B.A., Prospero J.M., Mackie D., Gaiero D., Hesse P.P., Balkanski Y., 2010. Global connections between Aeolian dust, climate and ocean biogeochemistry at the present day and at the last glacial maximum. Earth Science Reviews 99, 61-97.

Maher B.A., 2011. The magnetic properties of Quaternary Aeolian dusts and sediments, and their palaeoclimatic significance. Aeolian Research 3, 87–145.

Maher B.A., Thompson, R., 1995. Paleorainfall Reconstructions from Pedogenic Magnetic Susceptibility Variations in the Chinese Loess and Paleosols. Quaternary Research 44, 383-391.

McTainsh G. H., Walker P.H., 1982. Nature and distribution of Harmattan dust, Zeitschrift für Geomorphologie 26, 417–435.

NCEP, 1994. http//cpc.ncep.noaa.gov/products/special_summaries/94_2 (Figure 1).

Oldfield, F. 2012. Mud and magnetism: records of late Pleistocene and Holocene environmental change recorded by magnetic measurements. *Journal of Paleolimnology*. doi: 10.1007/s10933-012-9648-8.

Oldfield F., Hunt A., Jones M.D.H., Chester R., Dearing J.A., Olsson L., Prospero J.M., 1985. Magnetic differentiation of atmospheric dusts. Nature 317, 516-518.

Prospero J.M., Nees, R.T., 1977. Dust Concentration in the Atmosphere of the Equatorial North Atlantic: Possible Relationship to the Sahelian Drought. Science 196, 1196-1198.

Pye K., 1989. Processes of fine particle formation, dust source regions, and climatic changes. In Leinen, M., Sarnthein, M. (Eds.), Paleoclimatology and Paleometeorology: Modern and past patterns of Global Atmospheric Transport. Kluwer Academic Publications, Dordrecht, pp. 3-30.

Romero O.E., Lange C.B., Swap R., Wefer G., 1999. Eolian-transported freshwater diatoms and phytoliths across the equatorial Atlantic record: Temporal changes in Saharan dust transport patterns. Journal of Geophysical Research 104, 3211-3222.

Scheinost A.C., Chavernas A., BarrónV., Torrent J., 1998. Use and limitations of the second-derivative diffuse reflectance spectroscopy in the visible to near-infrared range to identify and quantify Fe oxide minerals in soils. Clays and Clay Minerals 46, 528–536.

Schlüter T., 2006. Geological Atlas of Africa, Springer, Berlin.

Schwertman U., Taylor R.M., 1989. Iron Oxides. In Dixon, J.B. and Weed, S.E. (Eds.), Minerals in Soil Environments 2nd Ed. Soil Science Society of America, Madison Wisconsin, USA, pp. 379–438.

Servant M. and Servant S., 1970. Les formations lacustres et les diatomées du Quaternaire Récent du fond de la cuvette Tchadienne. Revue de Géographie Physique et de la Géologie Dynamique 12, 63-73.

Shi, Z., Krom, M.D., Bonneville, S., Baker, A.R., Bristow, C., Drake, N., Mann, G., McQuaid J., Carslaw K., Jickells, T., Benning, L.G., 2011, Influence of soil weathering and aging of iron oxides on the potential iron solubility of soil dust during simulated atmospheric processing. Global Biogeochemical Cycles. 25, GB2010, doi:10.1029/2010GB003837.

Slingo, A., Ackerman, T.P., Allen, R.P., Kassianov, S.A., McFarlane, S.A., Robinson, G.J., Barbard, J.C., Miller, M.A., Harres, J.E., Russell, J.E., Dewitte, S. 2006. Observations of the impact of a major Saharan dust storm on the atmocpheric radiation balance. Geophysical Research Letters 33, L24817,doi:10,1029/2006GL02789,2006.

Tegen, I., Heinold B., Todd M., Helmert J,Washington, R., Dubovik O., 2006. Modelling soil dust aerosol in the Bodélé depression during the BodEx campaign. Atmospheric Chemistry and Physics 6, 4345-4359.

Torrent J., Barrón V., 2002. Diffuse reflectance spectroscopy of iron oxides. In Hubbard, A.T. (Ed.) Encyclopedia of Surface and Colloid Science, Taylor and Francis, New York, pp. 1438 – 1446.

Torrent J., Liu Q., Bloemendal J., Barrón, V., 2007. Magnetic Enhancement and Iron oxides in the Upper Luochuan Loess-Paleosol Sequence, Chinese Loess Plateau. Soil Science Society of America Journal 71, 1570 – 1578.

Vermeesch P., Leprince S., 2012. A 45-year time series of dune mobility indicating constant windiness over the central Sahara. Geophysical Research Letters 39, L14401, doi:10.1029/2012GL052592, 2012

Walden J., Oldfield F., Smith, J. 1999.(Eds.), Environmenmtal Magnetism: a practical guide. Quaternary Research Association, Technical Guide.

Washington R., Todd M.C., 2005a. Atmospheric controls on mineral dust emission from the Bodélé Depression Chad: the role of the low level jet. Geophysical Research Letters 32**,** L17701

Washington R., Bouet C., Cautenet G., Mackenzie E. , Ashpole I., Engelstaedter S., Lizcano G., Henderson G.M. Schepanski K., Tegen I.,2009. Dust as a tipping element: The Bodélé Depression, Chad. Proceedings of the National Academy of Sciences, USA 106 no. 49 20564-20571

Washington R., Todd M.C, Engelstaedter S., Mbainayel S., Mitchell F., 2005b. Dust and the low-level circulation over the Bodélé Depression, Chad: Observations from BodEx. Geophysical Research111, D03201, doi:10.1029/2005JD006502, 2006

Washington R., Todd M.C., Middleton N.J., Goudie A.S., 2003. Storm Source Areas Determined by the Total Ozone Monitoring Spectrometer and Surface Obsevations. Annals of the Association of American Geographers 9, 297–313.

Williams, E.R. 2008. Comment on ”Atmospheric controls on the annual cycle of North African dusts” by S. Engelstaedter and R.Washington”. Journal of Geophysical Research 113, D23109, doi:10.1029/2008JD009930, 2008.

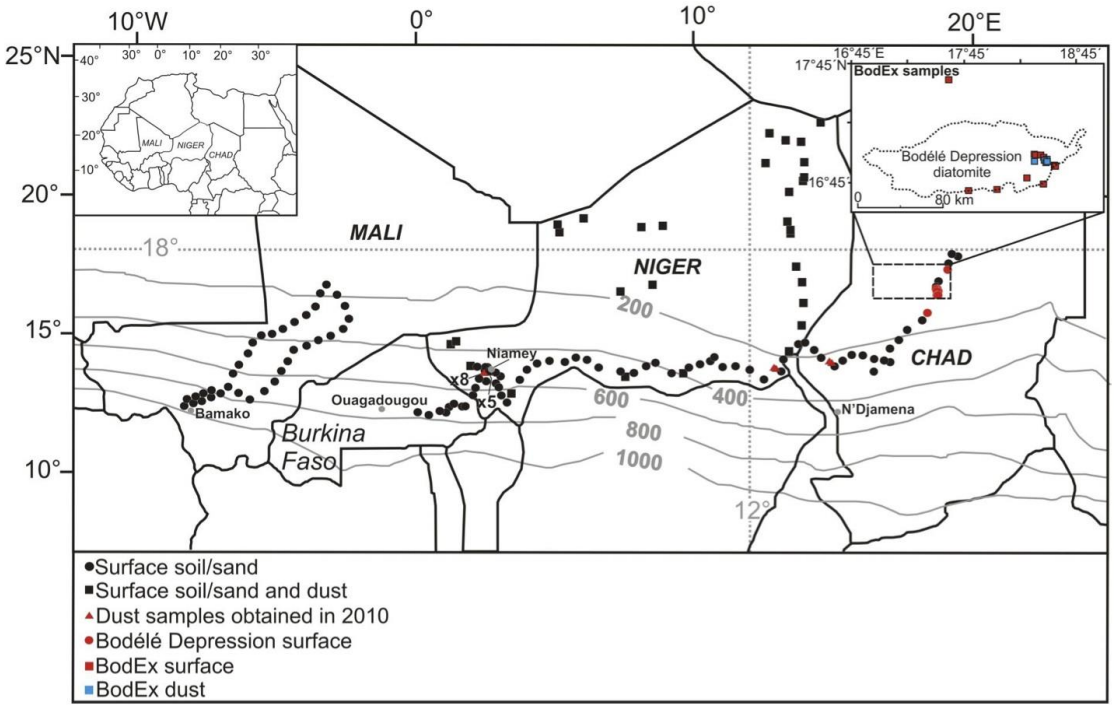

Figure 1. Location map of the sample sites in North Africa. The inset map (top right) shows the location of samples obtained during the BodEx Campaign, relative to the area of diatomite within the Bodélé́ Depression. The surface samples from the Mali transect (circles) were obtained in 2006 (Group 1); locations in Niger (squares) that yielded both surface (Group 1) and dust (Group 2) samples, were obtained in 2007. The samples from the Tansects through Burkina Faso, Niger and Chad (circles) were obtained in 2010 (Group 1). Within this set, the red circles represent Group 1b samples. The locations of the samples in Group 2c are shown by red triangles. The BodEx samples were obtained during the field campaign in 2005.

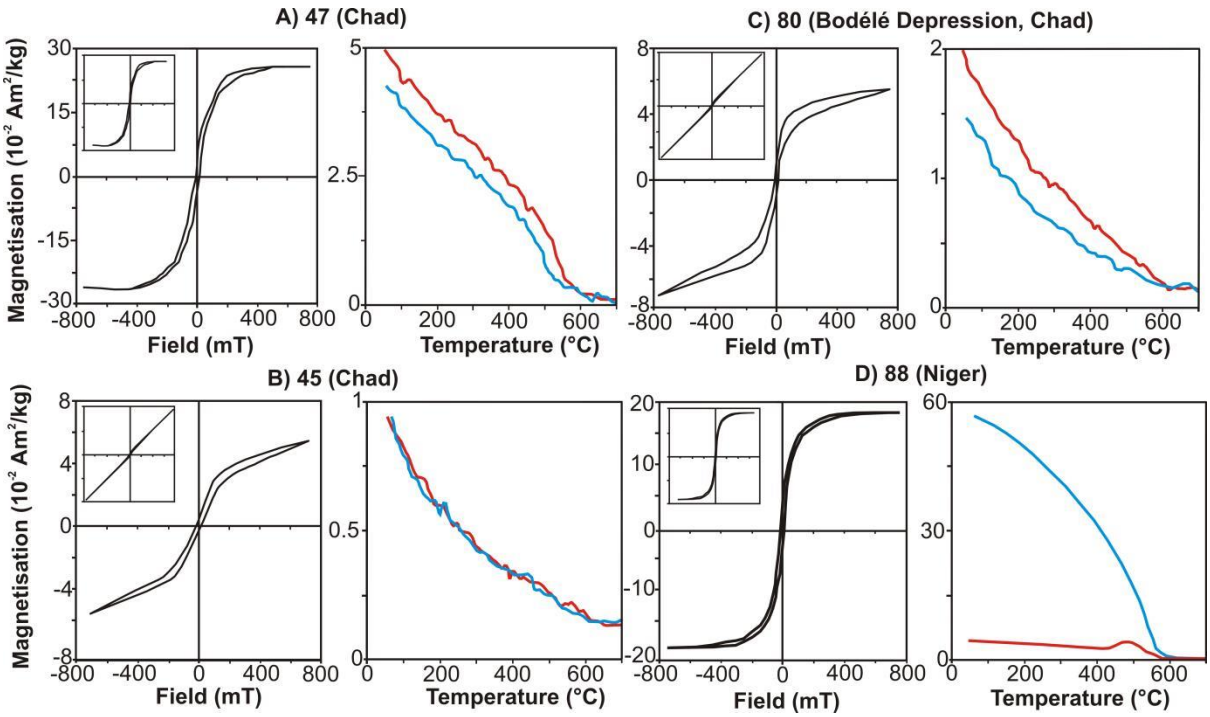

Figure 2. Four representative magnetic hysteresis and thermomagnetic curves. The main plots are slope corrected for paramagnetic effects, the insets, uncorrected. **2a** (Sample 47 from Group 1c: χ_{LF} = 6.04x10^{-8} m^3 kg^{-1}) represents a small number of samples from the arid area of Chad, close to the Bodélé Depression with χ_{LF} > 5 x 10^{-8} m^3 kg^{-1}. **2b** (Sample 45 from Group 1c: χ_{LF} = 0.74 x 10^{-8} m^3 kg^{-1}) represents more typical, weakly magnetic samples from the region. **2c** (Sample 80 from Group 1b: χ_{LF} = 5.3 x10^{-8} m^3 kg^{-1}) represents typical surface material from the Bodélé Depression sampled in 2010. **2d** (Sample 88 from Group 3: χ_{LF} = 125.6 x10^{-8} m^3 kg^{-1}) is a dust sample Niamey, Niger during Harmattan conditions in November 2009.

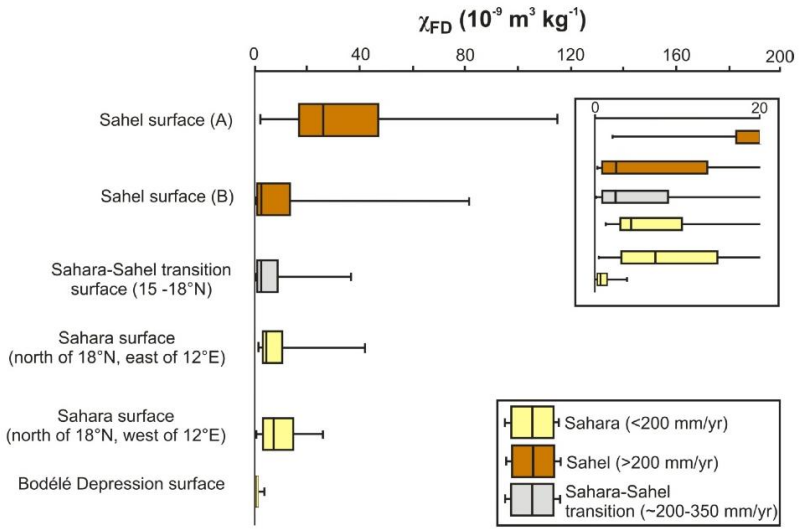

Figure 3a Box-whisker plot of χ_{FD} values for surface sample sets from North Africa (Group 1). The boxes show the 50th and 75th percentiles values, the 'whiskers' the maximum and minimum values. The inset is an expansion of the χ_{FD} values below 20 x 10^{-8} m^3 kg^{-1}. The Sahel set (A) (n=53) values are those from Lyons et al. (2012). The (B) (n=56) values represent samples collected in 2010 along an east-west transect from 16°E to 0°E and between 13°N and 15°N, close to the Sahara-Sahel transition. The Sahara surface samples east of 12°E (n=12) comprise Group 1a. The 'transition' group include those closest to the Bodélé Depression (Group 1c), from the most arid part of the 2010 transect. The values for the Bodélé Depression include the measurements on all the bulk samples obtained in 2010 (Group 1b; n=8), including those subsequently rejected as atypical of potential dust sources (see text). Values obtained for particle size fractions from the Bodélé Depression also fall within the same range.

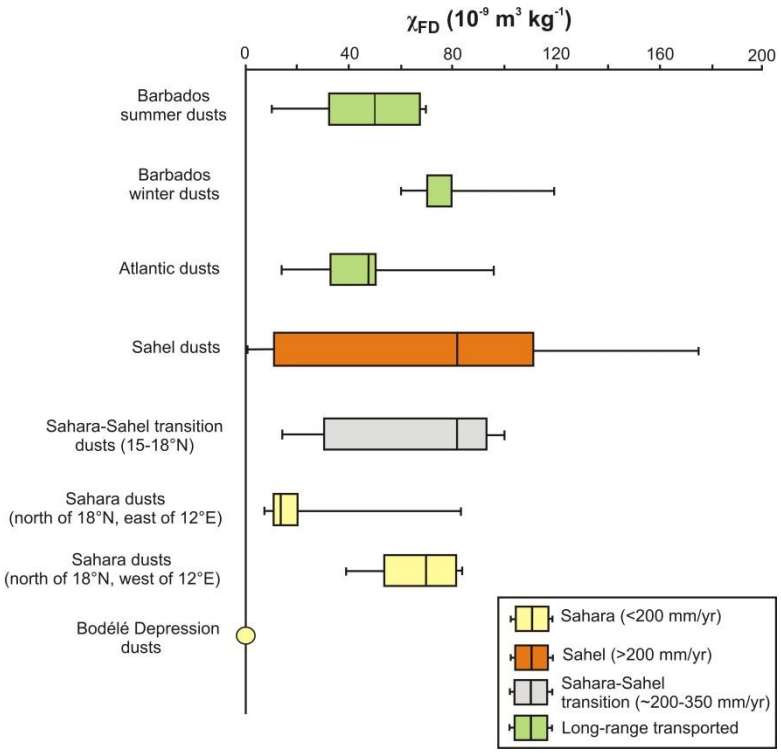

Figure 3b Box-whisker plot of χ_{FD} values for dust sample sets from North Africa, the North Atlantic unaffected by industrially generated particulates (Oldfield et al. 1985) and Barbados. The boxes show the 50th and 75th percentiles values, the 'whiskers' the maximum and minimum values. The values for the Barbados dusts (Group 4a; n=16) are from Oldfield et al. (1985). Those for the North Atlantic dusts (Group 4b; n=19) include data from samples described in the same publication, as well as from additional samples provided by R Chester and J.M.Prospero (see text). The Sahel (n=21), Sahara (n=16) and Transition (n=7) dusts (Group 2) come from the results in Lyons et al. (2012), and measurements on the Group 2b samples from Niamey (n=7) together with the dusts obtained in 2010 (Group 2c; n=5). As in the case of the surface samples, those taken from north of 18°N and east of 12°E (Group 2a; n=12) are from the most arid part of Niger. The zero value for the Bodélé Depression dusts is the mean of 10 measurements at each frequency on each of the 5 samples from the set obtained during the BodEx campaign in 2005 (Group 3).

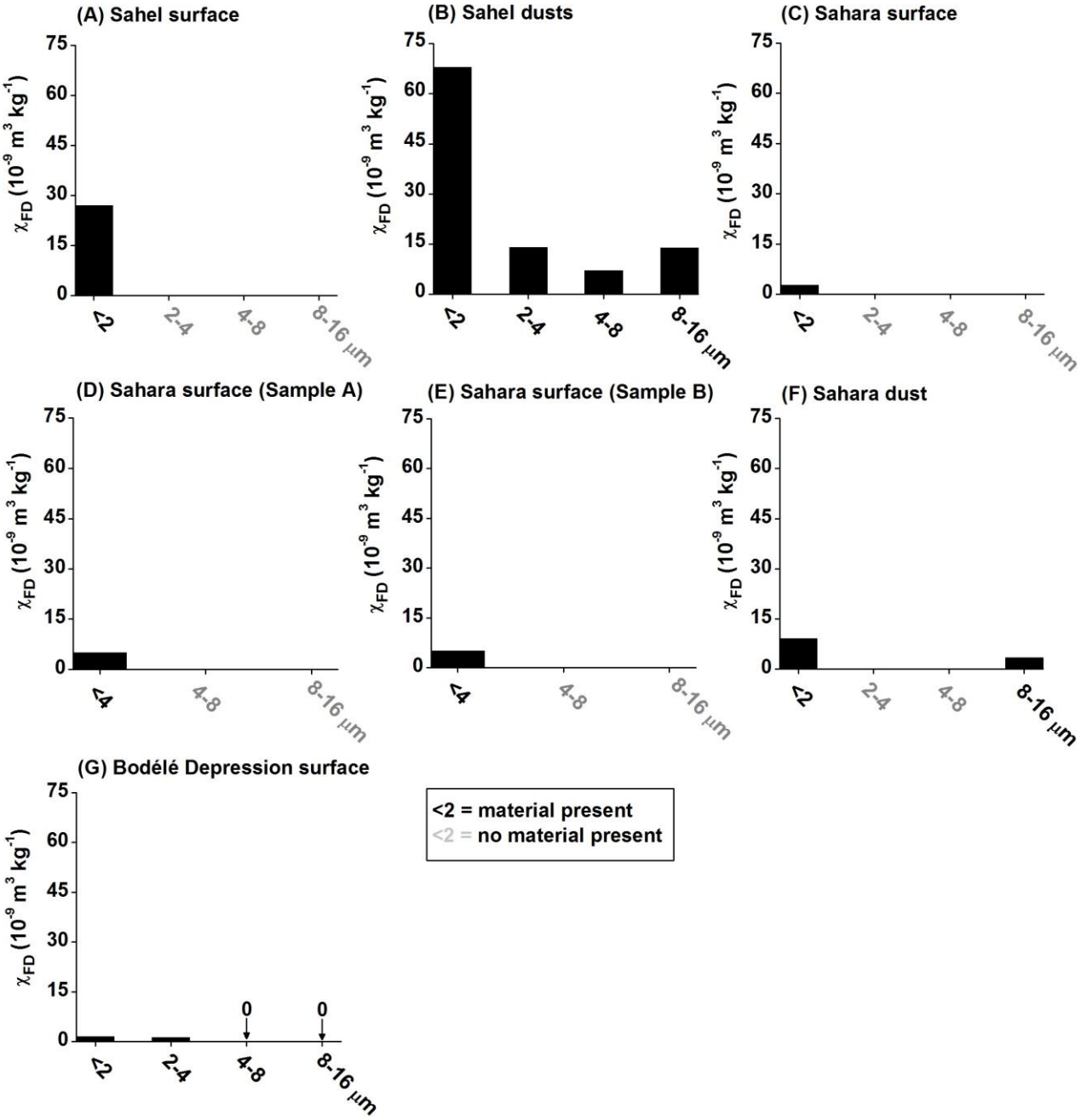

Figure 4. Plots of χ_{FD} values for particle sized samples. Histograms A and C are from Lyons et al. (2010); B and F are from Lyons et al. (2012). D and E refer to samples from Group 2; for both, too little material <2μm was extracted for reliable measurements. The values in G are the mean of samples 80, 81 and 82 and represent the mean of 15 readings at each frequency (5 for each subsample). D and E are based on 5 readings at each frequency and the remaining histograms are based on 3 readings at each frequency.

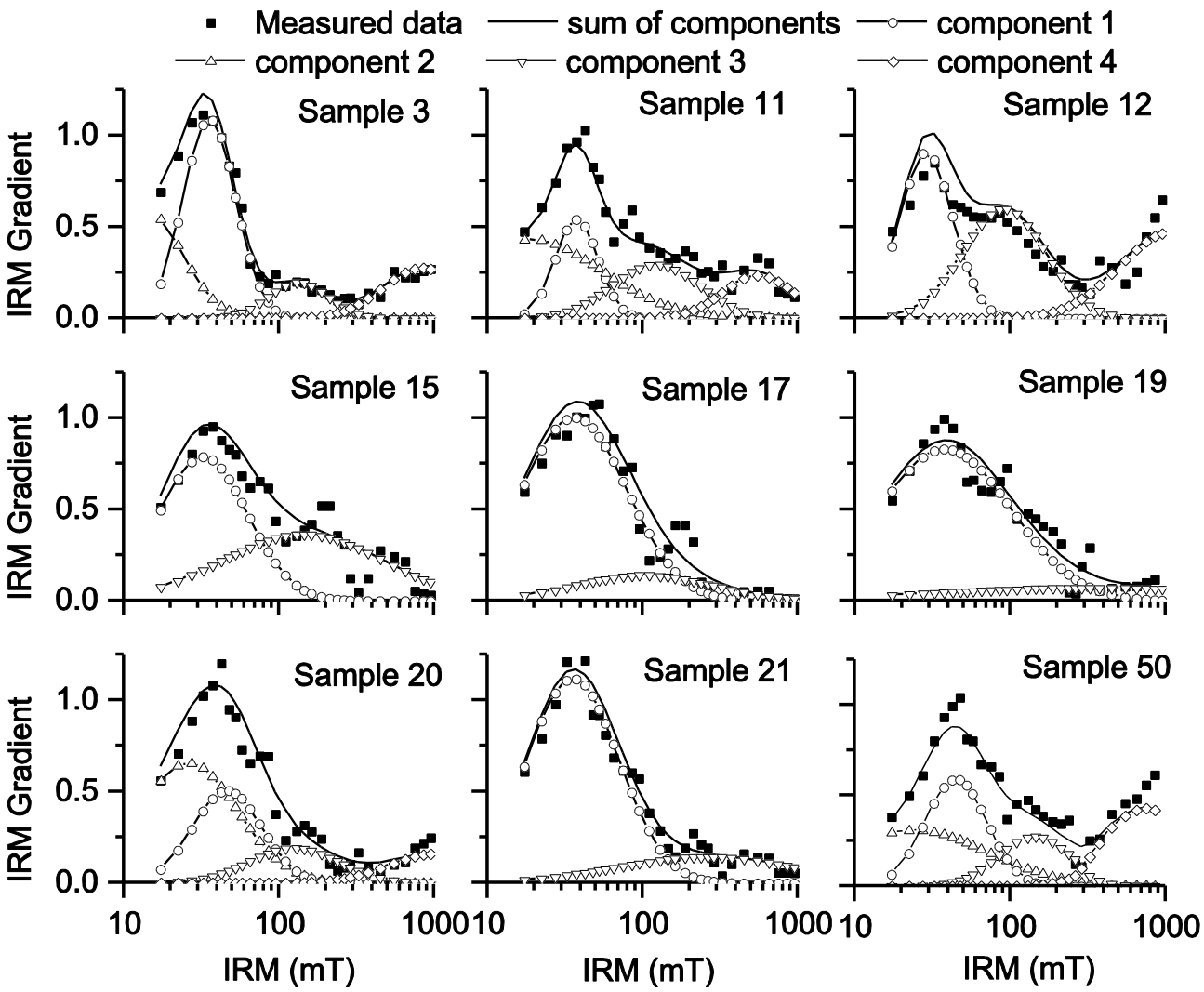

Figure 5. This and Figures 6 and 7 present the results of stepwise IRM acquisition up to 1T and subsequent model based de-convolution (Heslop et al. 2002) for selected representative samples. The key at the top applies to all three figures. All the samples used here are surface samples from the 2010 transect across Niger and Chad (Group 1). The peaks reflect the coercivity of different magnetic components in the sample. The analysis of the data is summarised in Table 3.

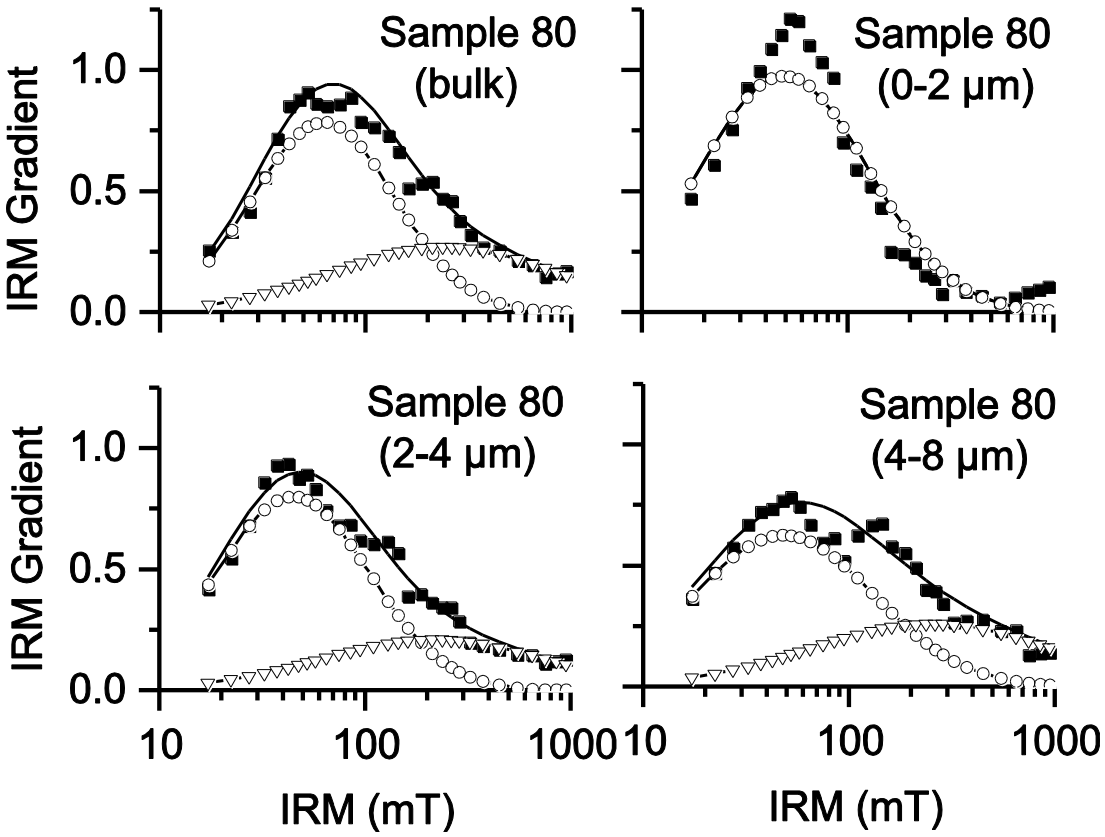

Figure 6. The results of stepwise IRM acquisition up to 1T and subsequent model based deconvolution (Heslop et al. 2002) for bulk and particle size fractions from surface sample 80 from the Bodélé Depression. The key to the symbols is given in Figure 5. The analysis of the data is summarised in Table 3.

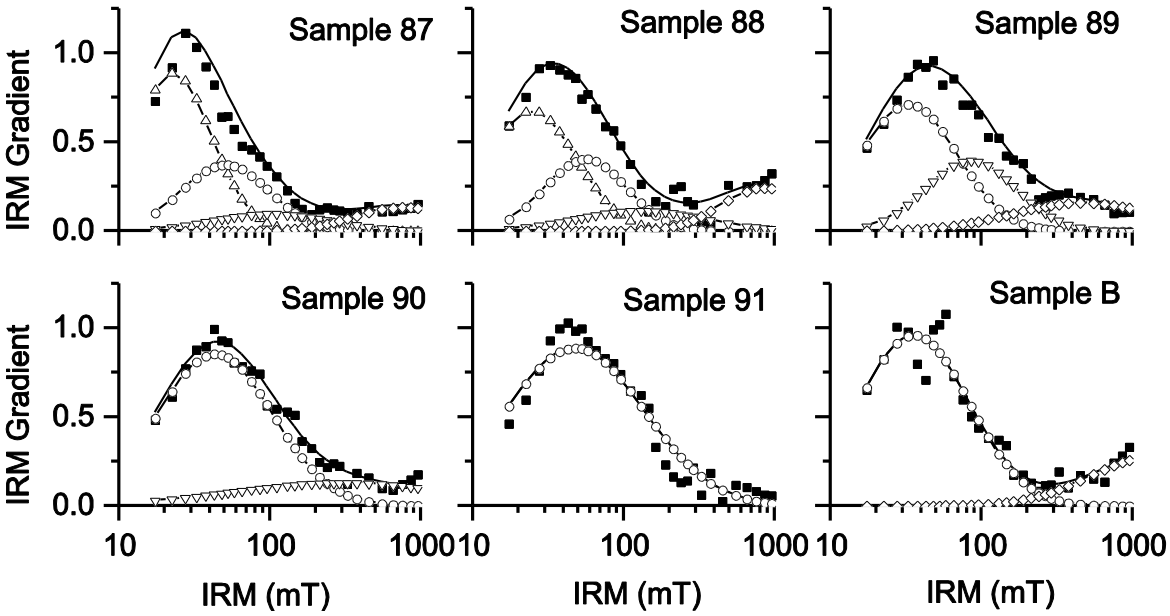

Figure 7. The results of stepwise IRM acquisition up to 1T and subsequent model based deconvolution (Heslop et al. 2002) for dusts from Niger and Chad obtained in 2009 (Group 3; samples 87 – 91) and for the <4μm fraction from a surface sample aggregated from 4 individual samples taken in 2010 from Niger and Chad (Group 1). The key to the symbols is given in Figure 5. The analysis of the data is summarised in Table 3.

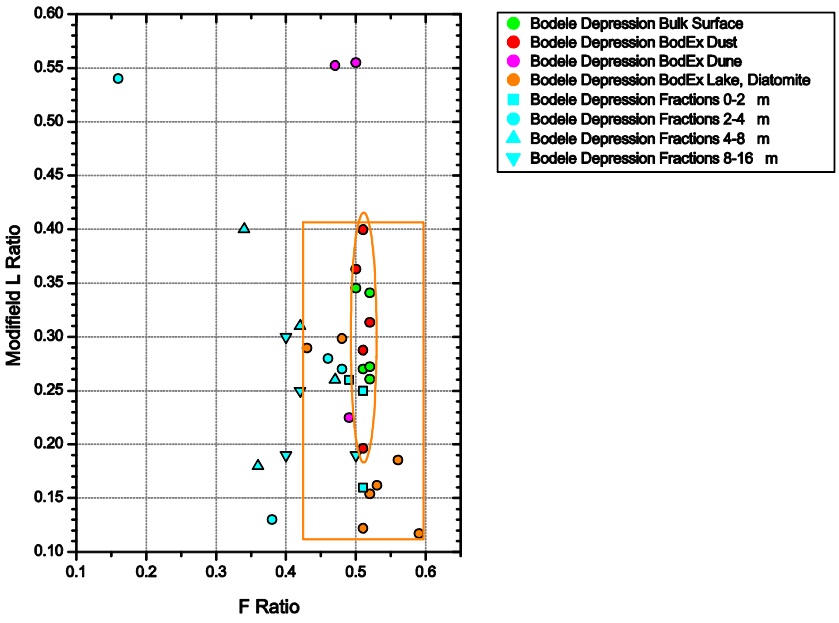

Figure 8. Cross-plot of two parameters derived from reverse field measurements on dusts and surface materials (both bulk and particle fractions) from the Bodélé Depression. Surface samples 83, 84 and 86 have been omitted (see text). The 'L' parameter is obtained by dividing the un-reversed IRM at -300mT by that un-reversed at -100mT. The F parameter is the difference between IRM_{-40mT} and IRM_{-20mT}, divided by the difference between SIRM and IRM_{-40mT}.The oval loop encloses the dusts and bulk sediment samples; the rectangle encloses, in addition, the surface lake sediment samples from the BodEx set as well as the particle size samples < 2 μm in samples 80, 81 and 82.

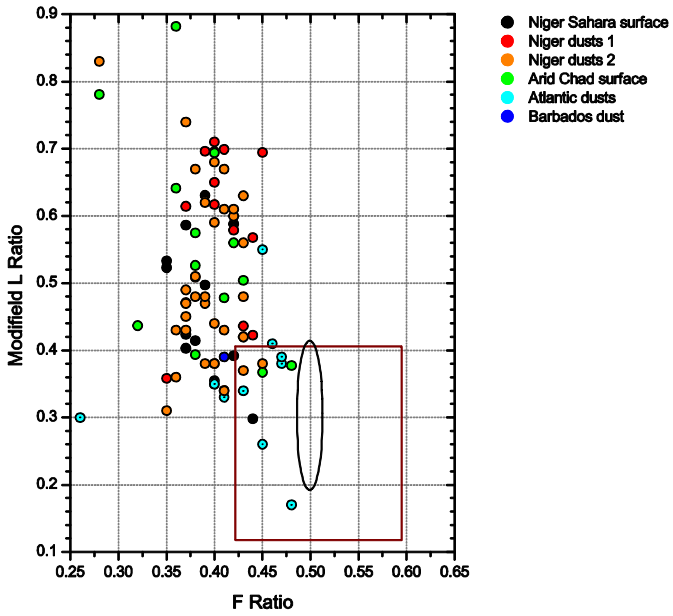

Figure 9. Cross-plot of two parameters derived from reverse field measurements on dusts and surface materials from a wide range of samples taken from outside the Bodélé Depression compared with the envelopes of values for the Bodélé Depression samples as defined in Figure 8.). The 'L' parameter is obtained by dividing the un-reversed IRM at -300mT by that un-reversed at -100mT. The F parameter is the difference between IRM_{-40mT} and IRM_{-20mT}, divided by the difference between SIRM and IRM_{-40mT}.The Niger Sahara surface samples are from Group 1a. The 'Arid Chad' surfaces are from Group 1c. The Niger dusts from Group 2a. are divided into 2 sets. The first comes from the arid north east part of Niger. The second set comes from sites that lie to the south and west of the Bodélé Depression from the zone that lies within the track of dust plumes from the Depression as indicated by remote sensing images (Washington et al. 2003; 2005 a and b) The only Atlantic Dusts from which the ratios could be calculated were those from Group 4b. The Barbados Dust sample is that taken in 1970 and provided by J. Prospero.

Sample Code	Sample type	Mass (g)	SIRM ($10^{-5}Am^2kg^{-1}$)	$S_{-0.02T}$ (%)	$S_{-0.04T}$ (%)	$S_{-0.1T}$ (%)	$S_{-0.3T}$ (%)
24 mid	Dust	0.204	278	27.3	56.6	89.7	96.8
26 mid	Dust	0.216	325	29.8	61.0	89.3	96.9
35 mid	Dust	0.193	326	28.5	57.7	90.7	98.2
36 mid	Dust	0.186	337	29.0	58.4	90.3	96.5
46 mid	Dust	0.126	479	27.1	55.4	89.9	96.0
CH8 Dia	Dune	1.707	72.9	28.4	53.3	79.9	88.9
CH9 Dia	Dune	2.175	65.9	29.3	57.5	86.3	96.9
CH15 Q	Dune	2.173	36.3	27.6	55.4	84.5	91.4
CH39 Ang	Lake	1.540	9982	36.9	66.1	92.0	99.6
CH62 BG	Lake	2.161	76.3	26.9	51.8	81.0	94.3
CH17	Diat	3.052	49.9	33.4	58.7	86.6	96.1
CH18	Diat	0.474	117	24.4	59.9	94.1	99.3
CH19	Diat	0.831	74.3	25.0	53.4	88.8	98.2
CH23	Diat	0.606	95.9	27.2	56.4	92.6	99.4
CH24	Diat	1.020	73.1	27.5	56.8	88.6	98.2
CH25	Diat	0.702	102	27.6	56.1	89.7	98.7
CH50	Diat	0.571	93.3	25.5	56.7	93.4	100.1
WPT 110	Soil	1.612	52.1	24.4	54.9	89.5	98.1
80_0-2	-	4.551	11.5	27.8	57.1	87.7	96.9
81_0-2	-	4.744	13.1	26.0	52.6	85.0	97.7
82_0-2	-	4.414	4.8	24.1	46.9	74.5	93.2
84_0-2	-	4.495	12.6	24.9	50.9	82.9	95.7
80_2-4	-	3.562	18.2	31.2	57.8	84.7	95.7
81_2-4	-	2.399	6.3	29.1	34.7	72.5	90.6
82_2-4	-	0.750	24.8	18.1	34.6	61.2	89.5
84_2-4	-	1.619	68.7	34.8	56.3	82.2	97.6
80_4-8	-	1.199	15.0	24.6	42.0	64.0	88.9
81_4-8	-	1.643	13.3	27.8	42.0	67.0	87.9
82_4-8	-	1.324	30.7	14.8	27.8	59.0	89.2
84_4-8	-	1.792	135	36.9	57.8	85.2	97.3
80_8-16	-	0.899	42.2	20.5	34.4	62.6	88.9
81_8-16	-	0.797	42.8	24.1	41.7	67.1	90.3
82_8-16	-	2.050	50.8	14.9	30.1	61.8	93.0
84_8-16	-	1.182	204	36.5	60.8	87.7	97.6
79 (43.5)	-	6.105	22.6	15.8	32.3	63.3	90.1
80 (44)	-	9.091	17.6	17.7	35.4	63.4	87.3
81(44B)	-	7.864	17.5	18.7	38.8	66.9	88.7
82(44C)	-	6.707	21.5	15.4	32.0	64.1	90.2
83(44D)	-	12.715	354	1.0	3.6	32.3	88.2
84 (51)	-	6.514	66.6	32.7	54.0	81.7	93.9
85 (54A)	-	6.969	20.1	15.9	33.2	64.0	90.6
86 (54B)	-	11.859	139	2.6	5.5	25.5	79.5

Table 1. Sample mass and selected magnetic properties for bulk samples and particle size fractions from the Bodélé Depression. Samples 24 mid (dust) to WPT 110 were collected during the BoDEx campaign in 2005 (Group 3). Diat.= diatomite. The remaining samples of surface material (80 – 86) were collected in 2010 (Group1). Only the latter contained enough material for particle size separation and the particle size range is given against each measured fraction. The codes used for these samples are the laboratory number and (the field sample number). The bulk measurements confirm that samples 83 and 86 are atypical; the magnetic properties of the >4μm fraction for Sample 84 are also atypical. (see text). These samples have been excluded from Table 2 and from Figures 9 and 10 for reasons given in the text.

Table 2 The range of SIRM values for all the sample sets from North Africa, the Atlantic and Barbados.

Source	Sample types	$10^{-5}Am^2kg^{-1}$
Bodélé Depression (3)	-BoDEx Dusts:	277 – 479
	- BoDEx Surface samples	6 – 26.5
	(2) -Bulk surface samples	17 – 23
Arid Niger/Chad (1)	Surfaces	6 – 96
Niger (S. and W) (1)	Surfaces	12 – 318
Niger/ Chad (2)	Dusts	169 – 1420
Barbados	(4a) Summer Dusts*	410 – 730
	(4a) Winter Dusts*	470 – 740
Mid-Atlantic	(4a) Dusts*	560 – 1000
	(4b) Dusts	73 – 3340

The numbers in brackets refer to the groups defined in the text.

* In the case of these samples measured in 1984, the highest DC field for imparting an IRM was 830mT (Oldfield et al. 1985).

Table 3. Analysis of the IRM acquisition results.

Sample		B1/2 (mT)	DP(mT)	RC	B1/2(mT)	DP(mT)	RC	B1/2(mT)	DP(mT)	RC	B1/2(mT)	DP(mT)	RC
Sahara surfaces (Figure 5)													
3		14	1.7	0.31	36	1.5	0.43	133	1.6	0.09	845	1.8	0.17
11		19	2.9	0.18	38	1.4	0.48	121	0.9	0.20	554	1.7	0.13
12		29	1.5	0.33	91	1.8	0.34	1083	2.2	0.33			
15		33	1.9	0.54	142	3.3	0.36						
17		36	2.2	0.85	103	2.7	0.15						
19		38	2.7	0.83	331	9.7	0.18						
20		26	2.1	0.48	46	1.7	0.26	124	1.9	0.13	1039	2.0	0.12
21		36	2.0	0.80	258	3.7	0.20						
50		24	3.0	0.34	45	1.6	0.27	142	1.7	0.15	847	1.8	0.25
Bodélé Depression (Figure 6)													
80	(Bulk)	63	2.2	0.65	242	3.6	0.35						
	(0-2μm)	49	2.6	1.00									
	(2-4μm)	45	2.4	0.72	216	3.6	0.28						
	(4-8μm)	48	2.7	0.64	252	3.9	0.36						
Dusts from 2009 (Figure 7)													
87		23	1.8	0.54	50	1.9	0.26	102	2.4	0.09	764	2.1	0.11
88		25	2.0	0.47	56	1.9	0.26	128	2.6	0.11	850	1.9	0.16
89		33	2.1	0.54	85	2.0	0.28	468	2.9	0.18			
90		43	2.4	0.78	296	5.2	0.22						
91		47	2.9	1.00									
Sahara Surface – particle size fraction (Figure 7)													
B	(0-4μm)	36	2.3	0.75	1389	2.7	0.25						

$B_{1/2}$ represents the applied field at which the mineral phase represented acquires half of its saturation IRM, i.e. the mean coercivity of that part of the IRM acquisition spectrum. The dispersion parameter (DP) represents one standard deviation of the log-normal distribution for each magnetic mineral component, thus expressing its coercivity distribution. The parameter RC records the contribution each component makes to the total IRM acquisition up to 1T. The B1/2 values are derived from the succession of peaks in the IRM acquisition diagrams (Figs. 5,6 and 7). Components with a B1/2 value of less than 70mT are likely to reflect the contribution from ferrimagnetic minerals (magnetite/maghemite), those with B1/2 values above 100mT and especially above 200mT are likely to reflect the contributions from imperfect anti-ferromagnetic minerals (hematite and, to a lesser extent, goethite).